

Unoccupied bulk and surface states on Ag(111) studied by inverse photoemission

S. L. Hulbert and P. D. Johnson

Physics Department, Brookhaven National Laboratory, Upton, New York 11973

N. G. Stoffel and N. V. Smith

AT&T Bell Laboratories, Murray Hill, New Jersey 07974

(Received 14 December 1984)

We present k -resolved inverse photoemission spectroscopy (KRIPES) results for Ag(111) in the $\bar{\Gamma}\bar{K}$ direction of the surface Brillouin zone. The spectra were taken as a function of electron energy and angle of incidence at a fixed photon energy (9.7 eV) of the emitted radiation. The crystal-induced surface state and the image-potential-induced surface state are observed with final-state electron energies at $\bar{\Gamma}$ in good agreement with a recently proposed multiple reflection model and with dispersion characterized by effective masses $m^* = 0.7m$ and $m^* \approx m$, respectively. The measured intensity of the surface state roughly follows a $\cos^2\alpha$ dependence, where α is the angle between the sample normal and the polarization vector of the detected photons. Transitions into bulk-derived final states are observed, with final-state electron energies ranging from E_F to $E_F + 20$ eV. The dispersions of these bulk-derived final states agree with very simple "empty-lattice isochromats" derived from free-electron bands of proper symmetry, as well as with results of a band-structure calculation based upon a combined interpolation scheme.

I. INTRODUCTION

Inverse photoemission may be used to study both bulk- and surface-derived features in the unoccupied region of the electronic band structure. Direct k -conserving transitions allow band mapping of the bulk states which complements similar information for the occupied region of the band structure derived from photoemission experiments. This variant of the technique is known as k -resolved inverse photoemission spectroscopy (KRIPES).

Unoccupied surface states have been identified on both metal and semiconductor surfaces. These surface states may be classified into two categories: those derived from the crystal potential due to its termination at the surface, and those derived from the long-range image potential which the electron experiences outside the surface. The former are of the "Shockley" or "Tamm" type, previously observed in numerous photoemission experiments whilst the latter, because of their proximity to the vacuum level, have only been observed using inverse photoemission.

An occupied Shockley-type surface state has been observed previously at the center of the zone on the Ag(111) surface in several photoemission experiments. Away from the center of the zone the state was found to disperse upwards towards the Fermi level before disappearing. In this paper we show that this state may be observed to continue its dispersion above the Fermi level. We also show that, as on other surfaces with similar band gaps, image states exist below the vacuum level. We examine the unoccupied bulk band structure and in Sec. V we present a simple empty-lattice isochromat model as an aid to the identification of the bands involved in these k -conserving transitions.

In Sec. II we give details of our experimental procedure and in Sec. III we show the results of different experiments. Surface-derived features are discussed in Sec. IV and those arising from bulk transitions in Sec. V. The conclusions of the paper are summarized in Sec. VI.

II. EXPERIMENTAL DETAILS

The two central elements of the experimental apparatus, the electron source and the photon detector, are described separately elsewhere.^{1,2} Briefly, the electron source^{1,3} utilizes a low-temperature ($\approx 800^\circ\text{C}$) BaO cathode emitter and features lens elements designed to minimize space-charge effects at low kinetic energy (< 10 eV) and provide a reasonable current into a well-focused beam (5° full angular spread). For 6 eV electron kinetic energy, sample currents of $\approx 5 \mu\text{A}$ are routinely achieved with the electron beam focused into an ≈ 1.0 -mm [full width at half maximum (FWHM)] spot providing $0.1\text{-}\text{\AA}^{-1}$ momentum resolution ($5\text{--}10 \mu\text{A}$ and 0.2\AA^{-1} for 20-eV electrons). As in all KRIPES experiments reported so far, the component of parallel momentum is varied by rotating the sample, which is held at ground potential. By convention, positive angles correspond to rotations toward the photon detector. The Geiger-Müller-type photon detector² collects less than 1% of the 2π sr flux from the sample in a band pass of ≈ 0.7 eV centered about 9.7 eV. With such a small solid angle subtended at the surface it is possible to observe spatial anisotropies of the emitted photons due to polarization effects.

Sample cleanliness was achieved by repeated Ar sputtering and annealing in ultrahigh vacuum. Low-energy electron diffraction (LEED) and Auger-electron spectroscopy were used to characterize the sample surface.

III. RESULTS

Figure 1 shows our KRIPES measurements on Ag(111) at $\hbar\omega=9.7$ eV as a function of electron incidence angle θ_e in the $\bar{\Gamma}\bar{K}$ azimuth. In this azimuth it is possible to check alignments and determine normal incidence by comparing spectra taken on opposite sides of the surface normal.

For $\theta_e \approx 5^\circ$, a prominent peak emerges above the Fermi level and disperses to higher energy for $|\theta_e| < 30^\circ$. This state is identified as the continuation above E_F of the occupied surface state (SS) previously observed in normal photoemission by Roloff and Neddermeyer⁴ and by Hansson and Flodström.⁵ The fact that we observe this surface state in inverse photoemission at the center of the zone, i.e., for normally incident electrons, is associated with the limited energy and angular resolution of the experiment. In the earlier photoemission experiments this state was observed to be less than 0.1 eV below the Fermi level.

The set of small peaks that disperse upward from $E_V - 0.7$ eV at $\bar{\Gamma}$ (approximately 3.75 eV with respect to the Fermi level) is identified with the $n=1$ component of a Rydberg series of image potential (IS) surface states, as previously reported for a number of other single-crystal surfaces.^{1,6-9} The strong peak just above E_F for $\theta=45^\circ$ and the smaller peaks above E_V in all of the spectra are attributed (as discussed below) to bulk-derived direct transitions. The dispersion of all of these features is plotted in Fig. 2.

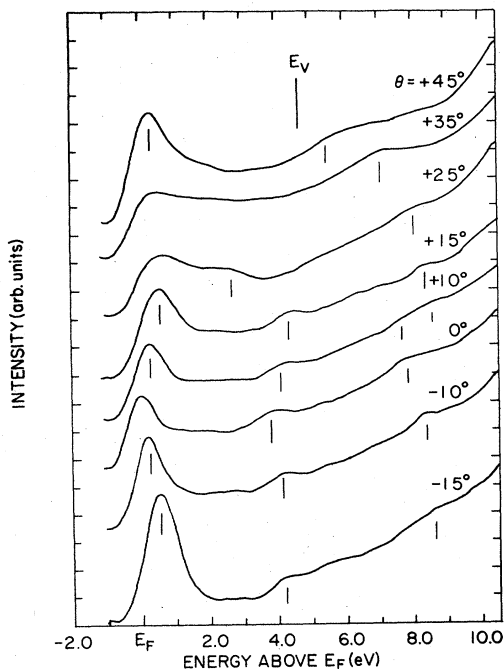


FIG. 1. KRIPES data for Ag(111) taken as a function of electron incidence angle in the $\bar{\Gamma}\bar{K}$ azimuth at $\hbar\omega=9.7$ eV.

IV. SURFACE-STATE DISCUSSION

We have recently demonstrated that a simple model based on multiple-reflection theory may be used to account for the binding energies of surface states found within band gaps at the center of the zone on low index faces of Cu.

This model considers surface states as electron waves trapped between a crystal barrier in the band-gap region and the barrier associated with the electron's image potential outside the surface. If $r_C e^{i\phi_C}$ and $r_B e^{i\phi_B}$ represent the respective amplitude reflectivities from these barriers, then bound or surface states correspond to poles of the function

$$\psi_+ = \{1 - r_C r_B \exp[i(\phi_C + \phi_B)]\}^{-1}. \quad (1)$$

A necessary condition for the existence of a surface state is therefore that the total phase change

$$\phi = \phi_C + \phi_B = 2\pi n, \quad (2)$$

where n is an integer.

We have shown that the image-potential-derived states form a Rydberg series with binding energies accounted for by this formula for $n \geq 1$. These binding energies relative to the vacuum level E_V are given by¹⁰ $e_n = (0.85 \text{ eV}) / (n + a)^2$, where the quantum defect $a = \frac{1}{2}(1 - \phi_C / \pi)$. We have further shown that the contribution $n=0$ in Eq. (2) leads to reasonable predictions for the binding energies of surface states or surface resonances derived from the crystal potential.

The phases in Eq. (2) are given by the expressions¹⁰⁻¹³

$$\phi_B = \pi \left[\left(\frac{3.4 \text{ eV}}{E_V - E} \right)^{1/2} - 1 \right] \quad (3)$$

and

$$\sqrt{E} \tan \left[\frac{\phi_C}{2} \right] = k_G \tan \delta - q, \quad (4)$$

where

$$2\delta = \sin^{-1} \left[\frac{Gq}{V_G} \right]. \quad (5)$$

Here G is the magnitude of appropriate reciprocal-lattice vector perpendicular to the surface, q is the imaginary part of the wave vector, and $2|V_G|$ is the width of the band gap. (See Refs. 10-13 for further details.) Solving Eq. (2) graphically, Fig. 3, we find that the first component of the series of image states should have a binding energy of 0.74 eV with respect to the vacuum level and the crystal-derived surface state should be found ≈ 0.04 eV below the Fermi level in the occupied region [the Ag(111) work function is taken to be 4.46 eV (Ref. 14)].

Experimentally we find that the image state has a binding energy of approximately 0.7 eV, which is close to the value predicted above. The dispersion of this state is found by least-squares fitting to be free-electron-like as expected. The crystal-derived surface state has been observed previously below the Fermi level in photoemission

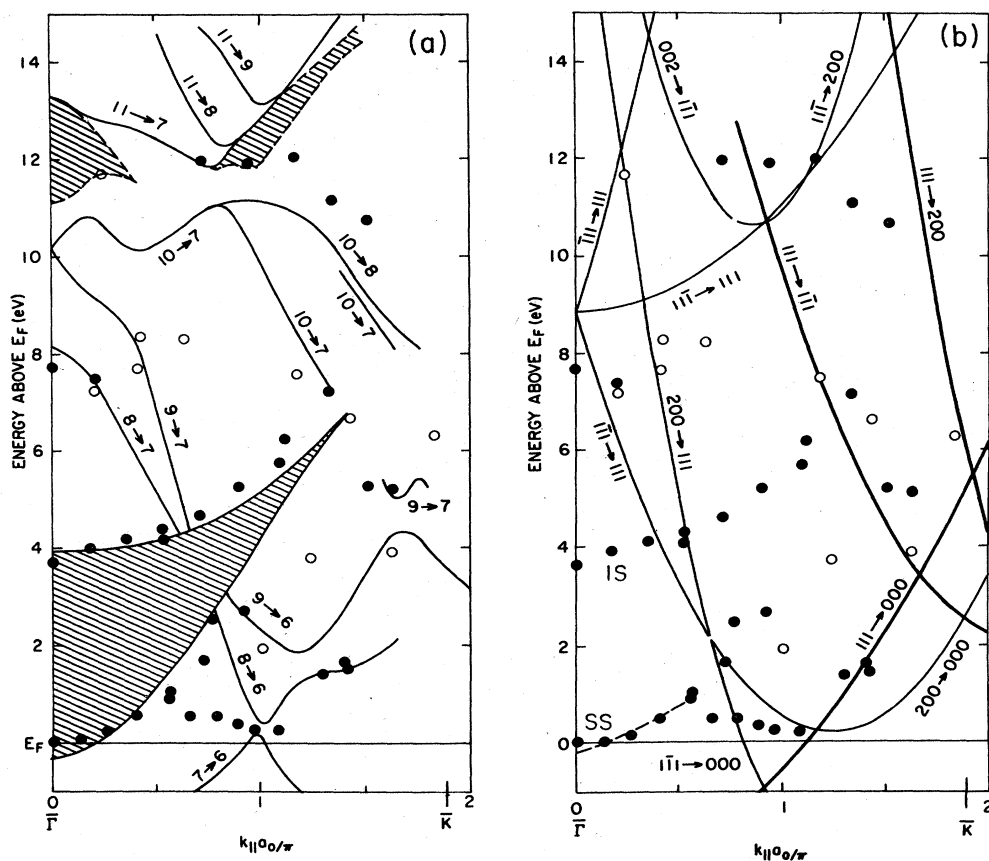


FIG. 2. Experimental and theoretical $E(k_{\parallel})$ dispersion relations for Ag(111) in the $\bar{\Gamma}\bar{K}$ azimuth. Cross-hatched area near E_F is the gap in projection of the bulk band structure. Cross-hatched areas near 12 eV are initial-state gaps shifted down by $\hbar\omega = 9.7$ eV. The crystal-induced surface state lies in the band gap near L_1^+ for $k_{\parallel} = 0$ and disperses with effective mass $m^* = 0.64m$. Dashed line in (b) is the dispersion calculated by Ho *et al.* (Ref. 15). The image-potential state follows a free-electron-like ($m^* \approx m$) dispersion. Remaining features are all bulk derived and are to be compared with (a) isochromats resulting from the combined interpolation scheme band-structure calculation (Ref. 17) and (b) the "empty-lattice" isochromats. The combined interpolation scheme band-structure isochromats are labeled by the initial- and final-state band indices; the empty-lattice isochromats are labeled by the reciprocal lattice vectors which identify the initial and final free-electron states. a_0 is the lattice parameter ($= 4.09 \text{ \AA}$).

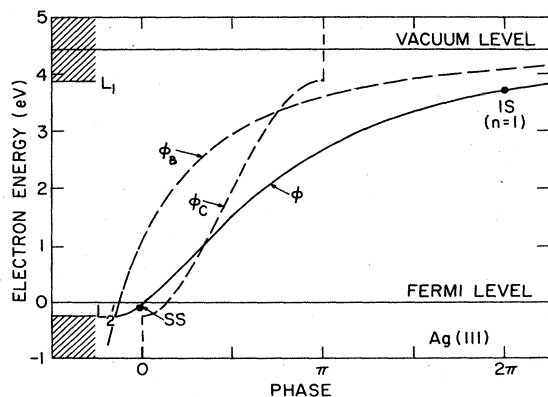


FIG. 3. Energy dependence of the phases ϕ_C , ϕ_B , and ϕ ($= \phi_C + \phi_B$) for the Ag(111) surface, which appear in the multiple-reflection theory of surface states (see Ref. 1 and references therein). Energy of the solid circle labeled IS is the observed binding energy of the $n = 1$ image-potential state. SS corresponds to the measured energy of the crystal-induced surface state on Ag(111) (Ref. 4).

experiments.^{4,5} Since this state is occupied at $\bar{\Gamma}$ it should not be observable at normal incidence in inverse photoemission. The fact that we do observe the state under such conditions is a reflection on the momentum resolution of our experiment. Figure 4 shows a plot of the intensity of the surface state as a function of the angle of incidence of the electrons. Derived from p_z -type orbitals, it would be expected that the intensity of emission from this state would show a $\cos^2 \alpha$ dependence where α is the angle between the photon polarization vector and the surface normal. The angle between the axis of the photon detector and the electron incidence direction is fixed at 45° and thus the expected $\cos^2 \alpha$ dependence translates into $\cos^2(\theta_e + 45^\circ)$ where θ_e is the electron incidence angle. Figure 3 shows reasonable agreement for this cross-section dependence for $-20^\circ \leq \theta_e \leq 40^\circ$. At angles less than -20° , grazing emission begins to limit the photon detection rate. Note that the intensity does show a minimum in the region of the surface normal, where the surface state has been observed below E_F .

Using the least-squares fitting procedure, the dispersion

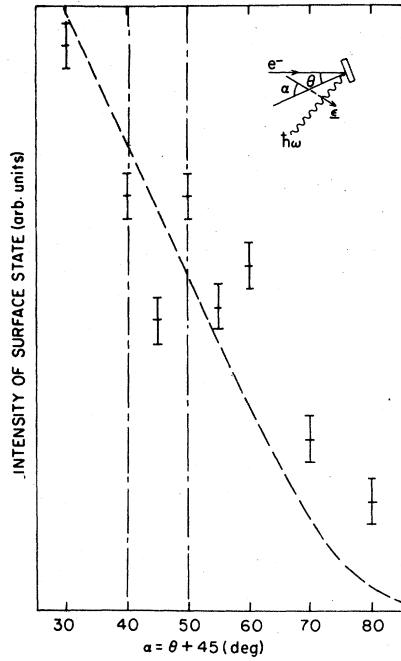


FIG. 4. Intensity of the crystal-derived surface state (SS) vs the angle α between the sample normal and the polarization vector ϵ of the detected photons. Angle between the axes of the photon detector and the electron gun is fixed at 45° , therefore $\alpha = \theta_e + 45^\circ$. SS intensity shows the expected $\cos^2 \alpha$ dependence (dashed line) as discussed in the text. Vertical dotted-dashed lines at $\theta_e \approx \pm 5^\circ$ mark the Fermi-level crossings of SS.

of this state is found to correspond to an effective mass of approximately $0.7m$, which is in good agreement with a first-principle calculation for this state by Ho *et al.*¹⁵ [dashed line in Fig. 2(b)]. The fitting procedure gives a binding energy ≈ 0.04 eV below the Fermi level at the center of the zone. As stated earlier, the value found from the model is also -0.04 , in excellent agreement with the experimental value. Previous photoemission experiments have found values of this binding energy ranging from -0.12 to -0.08 eV. There is therefore reasonable agreement between all experiments. However, it should be noted that a state lying so close to the Fermi level presents problems for all of the experiments relating to deconvolution of the Fermi function. We have also demonstrated elsewhere that the binding energy of these states depends upon the local work function.¹⁶

V. BULK BAND FEATURES

In addition to the surface features, a number of peaks are observed in the KRIPES spectra which arise from allowed transitions within the bulk band structure for Ag(111). The electron energies of the final states range from E_F to $E_F + 20$ eV. The (E, k_{\parallel}) positions for these measured peaks are plotted in Figs. 2(a) and 2(b): solid circles correspond to strong peaks, open circles to weaker features. The band gap in the projected bulk band structure is shown, and the SS and IS features discussed above are labeled. Superimposed on both Figs. 2(a) and 2(b) are

isochromats defined by

$$E_i - E_f - \hbar\omega = 0, \quad (6)$$

where E_i and E_f are the initial- and final-state energies (using a direct transition model) and $\hbar\omega$ is the energy of the emitted photons. In Fig. 2(a), E_i and E_f are determined using a combined interpolation scheme¹⁷ with the energies at the L'_2 and L_1 critical points constrained to the experimentally determined values.¹⁸ The agreement between the experimental points and the calculated isochromats is good. The experimental points at $E \approx E_F + 12$ eV are most likely associated with isochromats $10 \rightarrow 7$ and $10 \rightarrow 8$ which lie at ≈ 0.7 eV lower energy and below the gap in the initial states at $E \approx E_F + 24$ eV (shown shifted down by $\hbar\omega = 9.7$ eV, shaded regions within dashed outlines). Experimental points at $E - E_F = 8$ eV are associated with isochromats $8 \rightarrow 7$, $9 \rightarrow 7$, and $10 \rightarrow 7$ in that energy range. Below the final-state gap (L'_2, L_1) there is good correspondence between experimental points and bands $9 \rightarrow 6$ and $8 \rightarrow 6$.

In Fig. 2(b) we show "empty-lattice" isochromats determined within a free-electron model for Ag(111) for $\hbar\omega = 9.7$ eV. The initial-state and final-state energies are of plane-wave form:

$$E_i = (\mathbf{k} + \mathbf{G}_i)^2, \quad (7)$$

$$E_f = (\mathbf{k} + \mathbf{G}_f)^2, \quad (8)$$

where $\hbar^2/2m \equiv 1$ and \mathbf{G}_i and \mathbf{G}_f are the reciprocal-lattice vectors associated with the lowest-lying plane waves for the $[\bar{1}10]$ direction ($\bar{\Gamma}\bar{K}$) on the Ag(111) surface, namely (000), (111), ($1\bar{1}1$), (200), and ($1\bar{1}\bar{1}$). Eliminating k_{\perp} , the momentum component perpendicular to the (111) surface, the final-state energy is written as

$$E = (\mathbf{k}_{\parallel} - \mathbf{G}_{f\parallel})^2 + \frac{G_i^2 - G_f^2 - \hbar\omega - 2\mathbf{k}_{\parallel} \cdot (\mathbf{G}_{i\parallel} - \mathbf{G}_{f\parallel})}{2(G_{i\perp} - G_{f\perp})} - G_{f\perp}^2. \quad (9)$$

Initial states $\mathbf{G}_i = (111)$ should be most strongly coupled to the Ag(111) surface, i.e., isochromats with $\mathbf{G}_i = (111)$ should be most readily observed. The similarity between the empty isochromats and the isochromats derived from the combined interpolation scheme [Fig. 2(a)] permits assignment of the wave-function symmetries. For example, the combined interpolation scheme isochromat $10 \rightarrow 7$ is derived from empty-lattice isochromats ($11\bar{1} \rightarrow 111$) and ($111 \rightarrow 1\bar{1}1$), while isochromat $10 \rightarrow 8$ is derived from ($111 \rightarrow 200$). Both isochromats $10 \rightarrow 7$ and $10 \rightarrow 8$ contain significant (111) initial-state character and are therefore observable experimentally. The strongest bulk band feature is, as expected, derived from the ($111 \rightarrow 000$) isochromat.

VI. CONCLUSIONS

In this work we have again demonstrated the ability of inverse photoemission to provide information about the unoccupied states of a metal. We have shown that as in previous work¹ the binding energies of surface states may

be accounted for using a multiple-reflection model. We have measured the effective masses of all surface states at the center of the zone and in particular find good agreement with a first-principles calculation of the crystal-derived surface state on the same surface. The value of the effective mass that we have determined for the crystal-derived surface state on Ag(111) is higher than that previously found for the same state on Cu(111), the latter being 0.4 m . It should be noted however that the value for the Cu(111) surface was obtained from the measured dispersion close to the center of the zone. As one moves away from the zone center the parabolic dispersion of these states will gradually flatten out. Thus any effective mass derived from least-squares fitting will gradually increase as the dispersion is sampled farther out in the

zone.¹⁹

Bulk-derived features are interpreted in terms of both the combined interpolation scheme and a simple model based on a free-electron picture of the initial and final states. The latter method is therefore valuable for predicting the intensities of isochromats via their initial-state symmetries.

ACKNOWLEDGMENTS

We would like to acknowledge D. A. Wesner's assistance in some of the early stages of sample preparation. This work was supported by the Division of Materials Sciences, U.S. Department of Energy, under Contract No. DE-AC02-76CH00016.

-
- ¹S. L. Hulbert, P. D. Johnson, N. G. Stoffel, W. A. Royer, and N. V. Smith, *Phys. Rev. B* **31**, 6815 (1985).
²D. P. Woodruff, N. V. Smith, P. D. Johnson, and W. A. Royer, *Phys. Rev. B* **26**, 2943 (1982).
³N. G. Stoffel and P. D. Johnson, *Nucl. Instrum. Methods* **A234**, 230 (1985).
⁴H. F. Roloff and H. Neddermeyer, *Solid State Commun.* **21**, 561 (1977); P. Heimann, H. Neddermeyer, and H. F. Roloff, *J. Phys. C* **10**, L17 (1977).
⁵G. V. Hanson and S. A. Flodström, *Phys. Rev. B* **17**, 473 (1978).
⁶P. D. Johnson and N. V. Smith, *Phys. Rev. B* **27**, 2527 (1983).
⁷V. Dose, W. Altman, A. Goldman, U. Kolac, and J. Rogozik, *Phys. Rev. Lett.* **52**, 1919 (1984).
⁸D. Straub and F. J. Himpsel, *Phys. Rev. Lett.* **52**, 1922 (1984).
⁹D. A. Wesner, P. D. Johnson, and N. V. Smith, *Phys. Rev. B* **30**, 505 (1984).
¹⁰E. G. McRae, *Rev. Mod. Phys.* **51**, 451 (1979).
¹¹E. T. Goodwin, *Proc. Cambridge Philos. Soc.* **35**, 205 (1939).
¹²D. S. Boudreaux and V. Heine, *Surf. Sci.* **8**, 426 (1967).
¹³N. V. Smith, *Appl. Surf. Sci.* (to be published).
¹⁴Mahesan Chelvayohar and C. H. B. Mee, *J. Phys. C* **15**, 2305 (1982).
¹⁵K.-M. Ho, C.-L. Fu, S. H. Liu, D. M. Kolb, and G. Piazza, *J. Electroanal. Chem.* **150**, 235 (1983).
¹⁶D. P. Woodruff, S. L. Hulbert, P. D. Johnson, and N. V. Smith, *Phys. Rev. B* **31**, 4046 (1985).
¹⁷N. V. Smith, *Phys. Rev. B* **19**, 5019 (1979).
¹⁸L. Wallden and T. Gustafsson, *Phys. Scr.* **6**, 73 (1972); R. Rosei, C. H. Culp, and J. H. Weaver, *Phys. Rev. B* **10**, 484 (1974).
¹⁹M. Weinert (private communication).